THE EFFECT OF GEOMETRICAL CHARACTERISTICS OF DESICCANT WHEEL ON ITS PERFORMANCE

G. Heidarinejad* and H. Pasdar Shahri

Department of Mechanical Engineering, Tarbiat Modares University
P.O. Box 14115-143, Tehran, Iran
gheidari@modares.ac.ir – hadi.pasdar@gmail.com

S. Delfani

Building and Housing Research Center (BHRC)
P.O. Box 13145-1696, Tehran, Iran
delfani@bhrc.ac.ir

*Corresponding Author

(Received: November 28, 2007 – Accepted in Revised Form: September 25, 2008)

Abstract Desiccant wheels are widely used in buildings to control humidity and reduce energy consumption. A model is presented based on transient coupled heat and mass transfer, to model, design and analyze the effects of geometrical characteristics of a honeycombed rotary desiccant wheel and its performance. Governing equations are solved numerically using finite volume method and the model is validated using experimental measurements. It is shown that increasing desiccant wheel length will increase the latent and sensible effectiveness. Also, there is an optimum value for the ratio of dehumidification to regeneration area, which maximizes the latent heat effectiveness. Also the optimum hydraulic diameters of desiccant wheel channels depend on air mass flow rate.

Keywords Desiccant Wheel, Latent Effectiveness, Sensible Effectiveness, Numerical Simulation, Heat and Mass Transfer

چکیده از چرخ دسیکنت می‌توان برای کنترل رطوبت و کاهش مصرف انرژی در ساختمان استفاده کرد. در این مقاله مدل فیزیکی چرخ بر اساس آنالوژی انتقال حرارت و جرم ارائه شده است که به کمک آن می‌توان به طراحی و تحلیل مشخصه های هندسی آن بر عملکرد آن پرداخت. معادلات حاکم به کمک روش عددی حجم محدود حل و صحت نتایج بدست آمده با مقایسه آن با نتایج تجربی تایید شده است. نتایج نشان می‌دهد که با افزایش طول چرخ دسیکنت، بازده نهان و محسوس آن افزایش می یابد. همچنین مقدار بهینه‌ای برای نسبت رطوبت زدایی به احیا وجود دارد که مقدار بازده نهان در آن بیشینه است. مقدار بهینه قطر هیدرولیکی کانال‌های چرخ نیز به سرعت جریان هوا داخل آن بستگی دارد.

1. INTRODUCTION

In many buildings for air-conditioning processes, low humidity air is needed. In traditional methods to dehumidify air, the air is cooled to lower than its dew point, and it condenses part of its moisture which needs a lot of mechanical work. Also, more energy is required to heat the condensed air to obtain a suitable temperature. Another method to dehumidify air is the use of desiccant material which has high capacity to absorb moisture. All desiccants function by the same mechanism of transferring moisture because of the difference between water vapor pressure on the surface, and the surrounding air. When the vapor pressure at desiccant surface is lower than air, the desiccant absorbs moisture. When the surface vapor pressure is higher than that of the surrounding air, desiccant releases moisture [1]. This process occurs in a desiccant wheel alternatively. Therefore, desiccant wheels are frequently used to control humidity, create comfort conditions in air-conditioning systems and improves buildings indoor air quality (IAQ). Desiccant wheels are the heart of these

systems and have been widely used for air dehumidification and enthalpy recovery [2]. The humid air is dried after it flows through the wheel, which rotates continuously between the processed air and regenerative air stream.

Pesaran and Mills investigated the diffusion mechanism of moisture within silica-gel particle [3,4]. Their studies led to a model consisted of solid side resistance to fit the experimental data much better than pseudo-gas-side model. Van Den Bulck, et al introduced a cyclic analysis to establish a one-dimensional transient model of rotary heat and mass exchanger with infinite transfer coefficient employing ε-NTU method [5]. Zheng, et al used finite difference method to discuss the effect of rotational speed on the performance of desiccant wheel [6]. Majumdar investigated a composite desiccant dehumidifier made of mixed inert and desiccant materials [7]. His study revealed that the rate of desorption increases with the increase in fraction of inert material up to specific value. Simonson, et al developed dimensionless group and correlations to predict energy effectiveness of wheel [8,9]. Kodama, et al investigated desiccant wheel performance experimentally and developed functions to calculate optimum wheel rotational speed for two desiccant wheels with different dehumidification to regeneration surface area [10]. Niu, et al presented a two-dimensional coupled heat and mass transfer model which include both heat conduction, surface and gas diffusion in axial and thickness of wheel channels to predict and compare desiccant and enthalpy wheel [11,12]. Sphaier, et al developed and normalized a new dimensionless formulation to simulate both enthalpy exchangers and desiccant wheels [13]. Their studies show that within the range of real configurations for heat and mass Biot number, the temperature and mass gradient through the cross section (or thickness) of desiccant are small [14].

The aim of this paper is to develop a new transient model to study and analyze the effect of design parameters on the latent and sensible effectiveness of desiccant wheel. Practical approach led to variety of graphical presentation of the desiccant wheel performance in different geometrical design.

2. GOVERNING EQUATIONS

A rotary desiccant wheel is shown in Figure 1. It is a cylindrical rotating wheel of length L and radius R which is divided into adsorption section (Angle fraction α_0) and regeneration section (Angle fraction 2π-α_0). The regeneration and adsorption section are in the counter flow arrangement. Generally, the wheel contains parallel small channels and desiccant material typically constructed in its wall of usually sinusoidal or

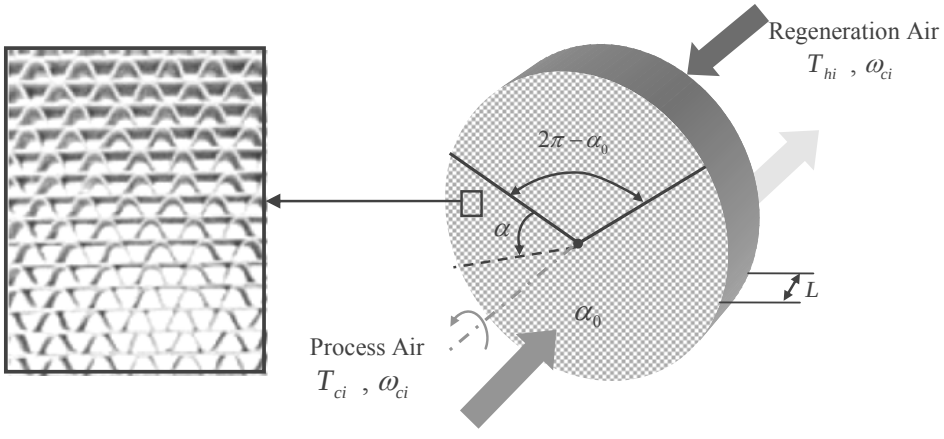

Figure 1. (a) Sinusoidal cross-sectional area and (b) schematic of desiccant wheel.

hexagonal cross-section. The desiccant percentage content f in thickness is usually about 70-80 (%). To simulate a desiccant wheel, assume a single channel as shown in Figure 2 which rotates continuously with speed of N(rpm) between adsorption and regeneration section. The channel cross-section and perimeter are A_{duct}, P_{duct} respectively.

The following assumptions are considered:

- No chemical reaction takes place in channels.
- The air flow in channels is incompressible.
- Heat and mass transfer along desiccant wheel and surrounding are negligible.
- The channel flow is laminar and fully developed.
- The specific heat and thermal conductivity of dry desiccant material are assumed constant.
- The concentration and porosity of sorption through channels are homogeneous.
- Heat and mass diffusion in radial direction are negligible.
- The rotary speed is uniform and low enough to neglect the effect of centrifugal force.

Based on the above mentioned assumptions a transient model is developed. The energy and mass conservation of air written as follow.

$$\rho_g C_{pg} \frac{\partial T_g}{\partial t} + u_g \rho_g C_{pg} \frac{\partial T_g}{\partial x} = \frac{4h}{D_h}(T_d - T_g) \qquad (1)$$

$$\rho_g \frac{\partial \omega_g}{\partial t} + \rho_g u_g \frac{\partial \omega_g}{\partial x} = \frac{4h_m}{D_h}(\omega_{eq} - \omega_g) \qquad (2)$$

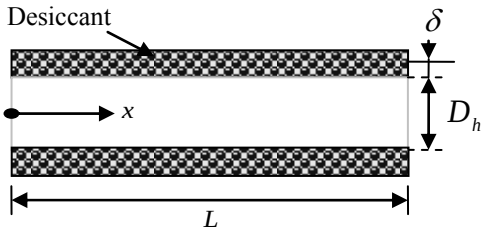

Figure 2. Single flow channel structure.

Also the energy and mass conservation of desiccant wheel can be written.

$$\rho_f C_{pf} \frac{\partial T_d}{\partial t} = \frac{\partial}{\partial x}(k_{eff} \frac{\partial T_d}{\partial x}) + \frac{h}{\delta}(T_g - T_d) + \frac{Q_{sor} h_m}{\delta}(\omega_g - \omega_{eq}) \qquad (3)$$

$$\rho_d \frac{\partial W_d}{\partial t} = \rho_d \frac{\partial}{\partial x}(D_s \frac{\partial W_d}{\partial x}) + \frac{h_m}{\delta}(\omega_g - \omega_{eq}) \qquad (4)$$

In the above four equations D_h is hydraulic diameter, h and h_m are convection heat transfer and mass transfer coefficients respectively. The system of equations can be completed by using sorption isotherm which depends on desiccant material. In this study the general sorption isotherm is used as defined below.

$$W_d = \frac{W_{max}}{1 - C + C/\phi} \qquad (5)$$

In Equation 5, ϕ is relative humidity near the surface of desiccant, C is the constant of isotherm which specify isotherm shape and W_{max} is maximum desiccant water content.

To compute the relative humidity and humidity ratio Equations 6, 7 and 8 are used [15].

$$\ln\left(\frac{P_{vs}}{22087.87}\right) = \frac{0.01}{T + 273.15}(374.136 - T). \sum_{i=1}^{8} F_i (0.65 - 0.01T)^{i-1}$$
$$F_1 = -741.9242; \quad F_2 = -29.7210$$
$$F_3 = -11.55286; \quad F_4 = -0.8685635$$
$$F_5 = 0.1094098; \quad F_6 = 0.49993$$
$$F_7 = 0.2520658; \quad F_8 = 0.05218684 \qquad (6)$$

$$\phi = \frac{p_v}{P_{vs}} \qquad (7)$$

$$\omega = 0.622\left(\frac{P_v}{P - P_v}\right) \qquad (8)$$

In above mentioned equations P_{vs} is saturation

vapor pressure which also depending on air and desiccant surface temperature respectively.

For regular density silica gel, heat of sorption is given by Pesaran, et al [3].

$$\begin{cases} Q_{sor} = 3500 - 13400 W_d & W_d \le 0.05 \\ Q_{sor} = 2950 - 1400 W_d & W_d > 0.05 \end{cases} \quad [\frac{kJ}{kg_{water}}] \tag{9}$$

3. THERMODYNAMIC PROPERTIES

Depend on air temperature, dry air density measured by Equation 10 [16].

$$\rho_a = \frac{1}{0.00283(T + 273.15)} \tag{10}$$

The density, thermal conductivity and specific heat of humid air and desiccant are given by the following equations:

$$\rho_g = \rho_a (1 + \omega_g) \tag{11}$$

$$C_{pg} = \left(\rho_a C_{pa} + \omega_g \rho_a C_{pv} \right) / \rho_g \tag{12}$$

$$k_g = \left(\rho_a k_a + \omega_g \rho_a k_v \right) / \rho_g \tag{13}$$

$$\rho_d = \rho_{d,dry} (1 + fW) \tag{14}$$

$$\rho_f = (1 - \varepsilon_f) \rho_d + \varepsilon_f \rho_g \tag{15}$$

$$C_{pf} = C_{pd} + W C_{pg} \tag{16}$$

$$k_{eff} = \left((1 - \varepsilon_f) \rho_d k_d + \varepsilon_f \rho_g k_{g,pores} \right) / \rho_f \tag{17}$$

The surface diffusion coefficient can be calculated using the following equation [3]:

$$D_s = \frac{D_0}{\tau} \exp(-0.974 \times 10^{-3} \frac{Q_{sor}}{T + 273.15}) \qquad D_0 = 1.6 \times 10^{-6} [m^2 s^{-1}] \tag{18}$$

Where, τ is tortuosity factor which is accounted for modifying surface diffusivity in rough walls of porous media.

To calculate heat and mass transfer coefficient, a laminar flow in channels is assumed. So Nusselt number and heat transfer coefficient can be calculated using the following equation [17].

$$Nu = \frac{4.36 \pi D_h^2}{4 A_{duct}} \tag{19}$$

$$h = \frac{Nu.k_g}{D_h} \tag{20}$$

The relation between h and h_m can be expressed by Lewis number.

$$h_m = \frac{h}{LeC_{pg}} \tag{21}$$

In the above equation, $Le = 1$ [11,12].

4. BOUNDARY CONDITIONS

The single simulated channel rotates between two air streams, so the boundary condition for gas side depends on channel position. During dehumidification, boundary conditions are:

$$\begin{cases} T_g(0,t) = T_{ci} \\ \omega_g(0,t) = \omega_{ci} \end{cases} \quad 0 \le \alpha < \alpha_0 \tag{22}$$

During regeneration, boundary conditions are:

$$\begin{cases} T_g(L,t) = T_{hi} \\ \omega_g(L,t) = \omega_{hi} \end{cases} \quad \alpha_0 \le \alpha < 2\pi \tag{23}$$

At $x = 0$ and $x = L$ the transfer areas correspond to less than 0.1 % of total. Thus, one may assume insulated and impermeable boundaries at these two ends with negligible errors [13], therefore:

$$\left.\frac{\partial T_d}{\partial x}\right|_{x=0} = \left.\frac{\partial T_d}{\partial x}\right|_{x=L} = 0$$
$$\left.\frac{\partial W_d}{\partial x}\right|_{x=0} = \left.\frac{\partial W_d}{\partial x}\right|_{x=L} = 0 \quad (24)$$

The output air temperature and humidity ratio are obtained after quasi steady time is reached. Therefore, the average exit temperature and humidity ratio during dehumidification are calculated as the following:

$$T_{g,out} = \frac{\int_0^{\alpha_0} T_g(\alpha, L)d\alpha}{\alpha_0} \quad (25)$$

$$\omega_{g,out} = \frac{\int_0^{\alpha_0} \omega_g(\alpha, L)d\alpha}{\alpha_0} \quad (26)$$

The latent effectiveness is defined as

$$\varepsilon_L = \frac{\omega_{ci} - \omega_{g,out}}{\omega_{ci}} \quad (27)$$

Sensible effectiveness is also defined as

$$\varepsilon_s = \frac{\dot{m}_p}{\dot{m}_{min}} \frac{T_{ci} - T_{g,out}}{T_{ci} - T_{hi}} \quad (28)$$

Where, $\dot{m}_p$ is the process mass flow and $\dot{m}_{min}$ is the least value of adsorption and regenerative mass flows. It must be mentioned that, for desiccant wheels which is used in desiccant cooling cycles, lower ε_s and higher ε_L results in better cycle performance. So, in this study, the effect of parameters on the sensible effectiveness also measured. Also, θ as dimensionless angle is defined as:

$$\theta = \frac{\alpha}{2\pi} \quad (29)$$

Where, α shows the angle of single channel from the start point of dehumidification part.

5. NUMERICAL METHOD

The system of conservation Equations 1-4 in which time and space variation are included can be integrated using finite volume method. For Equations 1 and 2 upwind methods and for diffusion term in Equations 3 and 4 central differences are used. To compute quasi steady state, fully implicit scheme is invoked because of its reliability and convergence. Finally, a TDMA solver is adopted to solve the set of linear algebraic equations for a uniform grid in x-direction. Necessary mesh independency and selection of time step were conducted before the final simulation to be done.

6. VALIDATION

To validate the model, several comparisons between experimental measurements by Kodama, et al [10] and numerical simulation was conducted. In experimental study, a honeycomb adsorbent rotor consisting of silica gel is used. Its width is20 cm, the silica gel wall thickness is 0.2 mm and contains 70-80 (%) of silica gel with sufficient rigidity. The equilibrium amount adsorbed for this wheel is $W = 0.24\phi^{1/1.5}$. Input air temperature and humidity ratio are 30˚C and 0.008 kg_W / kg_{DA}. Also, regeneration air temperature in experiment is 80˚C. Figure 3 shows the comparison between numerical results and experimental data. Despite the lack of experimental data, there is a good agreement between numerical results values and experimental data. The result shows that the prediction adsorption outlet air humidity ratio is less than the humidity ratio in experimental results. It is due to delay time between process and regeneration which decreases the time of dehumidification and regeneration. Also it is found that the prediction for output air temperature match with experimental data with errors less than 2 %. This error is due to humidity ratio results because the humidity ratio is predicted less than its actual

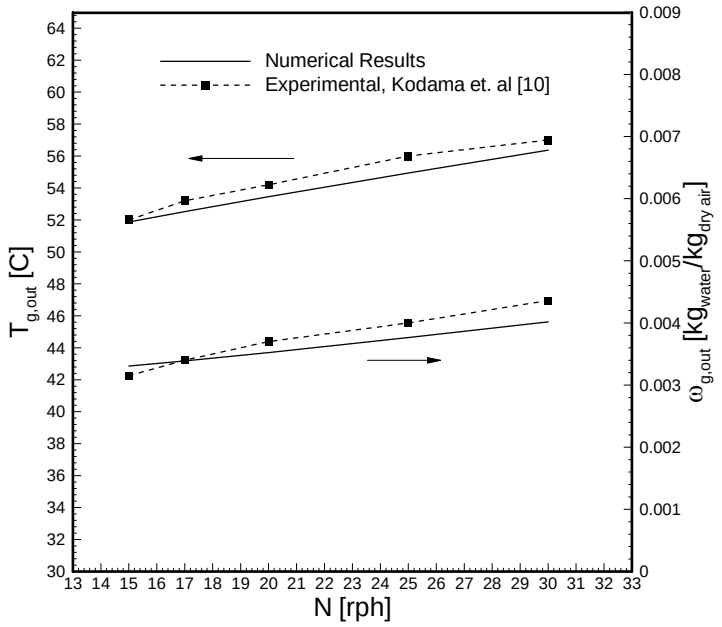

Figure 3. Comparison between predicted results and experimental data.

value and results in lower heat sorption and output air temperature.

7. RESULTS AND DISCUSSION

Air and water properties and data geometry are listed in Table 1. The cross sectional shape of desiccant wheel is sinusoidal with 2.5 mm height and4.2 mm base width. The perimeter and surface of channel is shown in Table 1.

Figure 4 shows the variation on outlet air humidity ratio from channels during dehumidification and regeneration in quasi-steady state. It can be seen that, at the beginning of dehumidification, the outlet air humidity ratio decreases down to $\theta \cong 0.1$. As channels rotate, in dehumidification section the rate of water adsorption reduces. It is due to drop in potential of desiccant material by adsorbing moisture. During regeneration process, air humidity ratio increase because of mass transfer between desiccant surface and regeneration air stream. Also Figure 4 shows the rate of desiccant regeneration decrease. Because of the surface vapor pressure drops with loss of moisture and reduction difference between vapor pressure of air stream and desiccant surface, the rate of mass transfer decreases. Therefore, the outlet air humidity ratio from wheel and latent effectiveness becomes $\omega_{g,out} = 6.48\,gr_w / kg_{DA}$ and $\varepsilon_L = 0.56$ respectively.

The effects of desiccant wheel length on the latent and sensible effectiveness are shown in Figures 5 and 6. The rate of the heat and mass transfer increases with length because it results in more area for heat and mass transfer so the latent and sensible effectiveness rises. For instance, by increasing the wheel length from 0.1m to 0.12m, the latent effectiveness rises approximately 8 %, while, increasing the channel length from 0.22 m to 0.24 m, the latent effectiveness increases close to % 1. This value can be checked by Figure 5. For instance, by 70 % outdoor relative humidity, the effectiveness increases from 0.46 to 0.47. It must be considered that desiccant wheel length can be extended up to an optimum value because more wheel length causes more pressure drops.

Desiccant wheel can be used with different ratio of dehumidification to regenerate surface area. This ratio has direct effects on the mass flow rate

TABLE 1. Common Input Data use in Simulation.

Symbol	Unit	Value	Symbol	Unit	Value
C_{pa}	[J/kg˚C]	1007	τ_s	[1]	3.0
C_{pv}	[J/kg˚C]	1870	ε_f	[1]	0.3
C_{pw}	[J/kg˚C]	4179	δ	[m]	0.1×10^{-3}
C_{pd}	[J/kg˚C]	920	W_{max}	$[kg_w / kg_{DD}]$	0.25
k_a	[W/m˚C]	0.0263	f	[1]	0.75
k_v	[W/m˚C]	0.0196	α_0	[rad]	π
k_d	[W/m˚C]	0.11417	P_{duct}	[m]	0.01137
ρ_d	[kg/m^3]	1129	A_{duct}	[m^2]	5.250×10^{-6}
u_p	[m/s]	2	u_{reg}	[m/s]	2
T_{ci}	[˚C]	30	T_{hi}	[˚C]	80
ω_{ci}	$[gr_w/kg_{DA}]$	12.5	ω_{hi}	$[gr_w / kg_{DA}]$	12.5

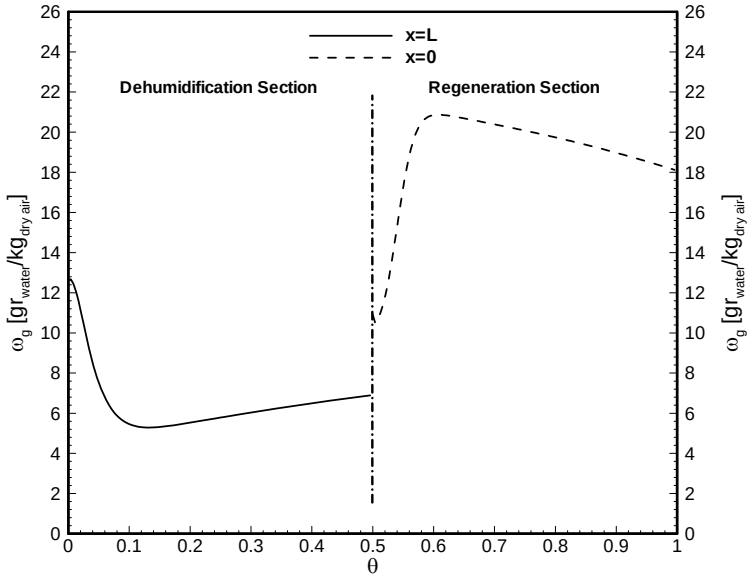

Figure 4. Output air humidity ratio during dehumidification and regeneration section.

which is used in both sections. The effects of the ratio of dehumidification to the whole wheel surface area on the latent and sensible effectiveness of desiccant wheel for T_{hi} = 80˚C are shown in Figures 7 and 8 respectively. Both regeneration and dehumidification air speed are assumed to have equal values. It can be seen that there is an optimum value for which the maximum value of latent effectiveness can be obtained. These optimum values also depend on wheels' rotational speed.

Actually in optimum values, dehumidification

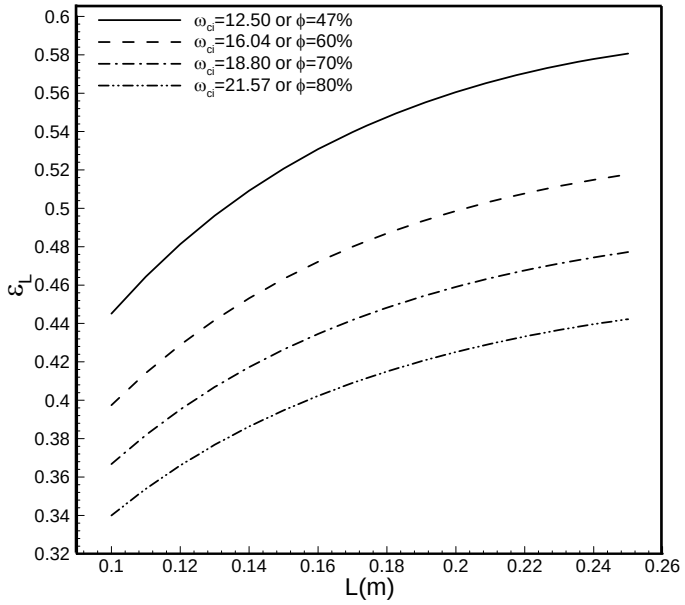

Figure 5. Latent effectiveness under various desiccant wheel lengths.

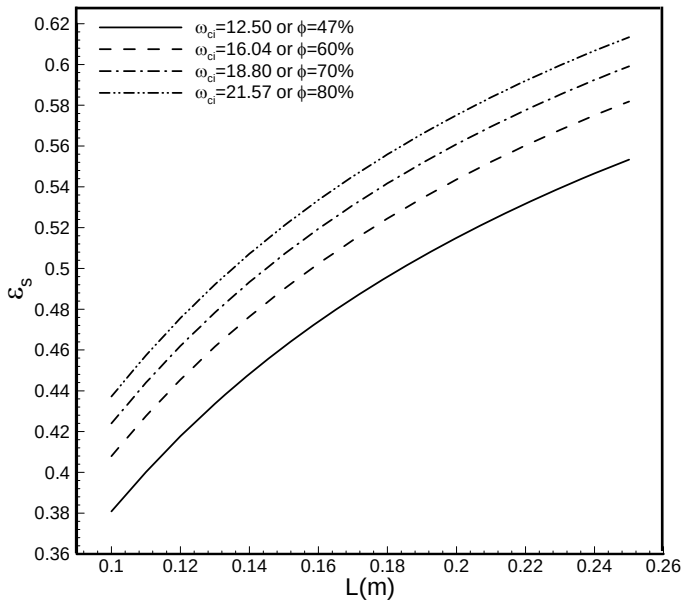

Figure 6. Sensible effectiveness under various desiccant wheel lengths.

of air and regeneration of desiccant in channels occurs on its best form because the times of both processes are sufficient. On the other hand, when the rotational speed rises, more time is needed for regeneration so the ratio is increased.

Figure 8 shows that in all rotational speed, when the ratio of dehumidification to regeneration is increased, sensible and latent effectiveness

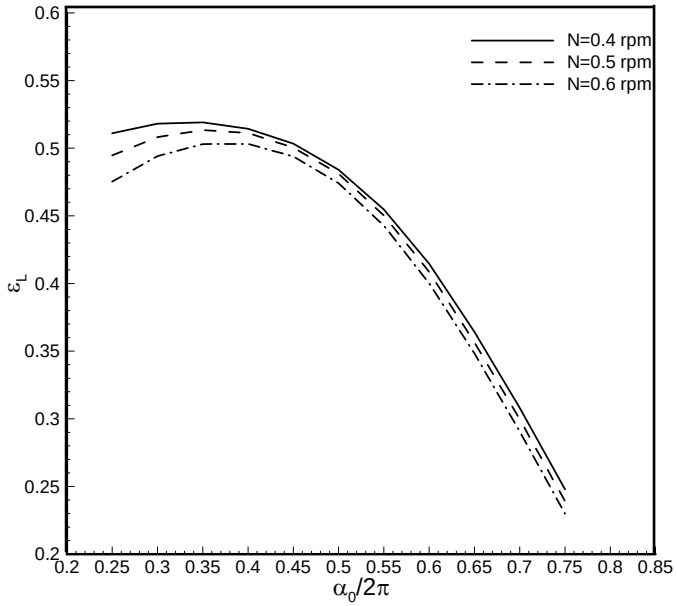

Figure 7. The effect of ratio of dehumidification to whole surface area on latent effectiveness.

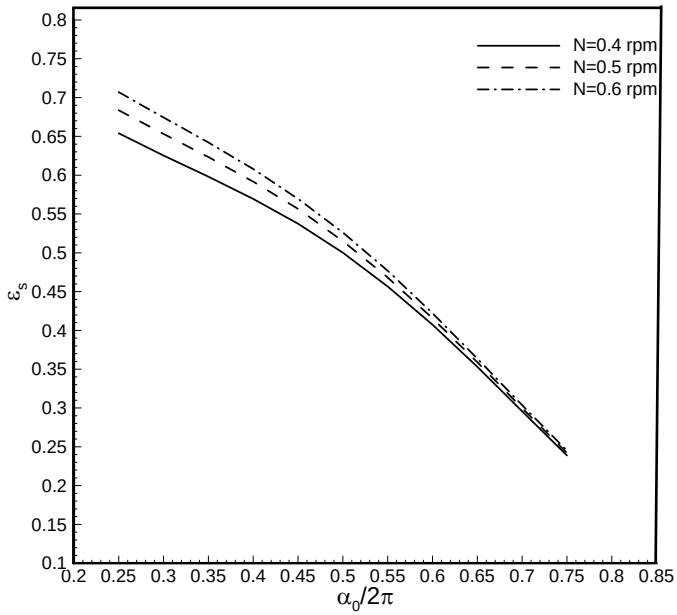

Figure 8. The effect of ratio of dehumidification to whole surface area on sensible effectiveness.

drops. Depending on the initial assumptions, the air velocity in channels in both regeneration and dehumidification sections are the same. Therefore, the more $\alpha_0/2\pi$ results in more process air mass flow rate and reduce the outlet air temperature.

The comparison between outlet air humidity

ratio ($\omega_g(\theta,L)$) from one channel during dehumidification section and $\omega_{g,out}$ for $\frac{\alpha_0}{2\pi}=0.4$ and $\frac{\alpha_0}{2\pi}=0.65$ with N = 0.5 rpm are shown in Figure 9. The maximum value of latent effectiveness can be obtained in $\frac{\alpha_0}{2\pi}=0.4$. Figure 9 shows that at the end of dehumidification section with $\frac{\alpha_0}{2\pi}=0.4$, the value of outlet air humidity ratio becomes $\omega_{g,out}$. This shows that air dehumidifying in this case is optimum but in $\frac{\alpha_0}{2\pi}=0.65$ the outlet air humidity ratio at the end of dehumidification process is more than $\omega_{g,out}$. This shows the ability of desiccant material at the end of dehumidification to adsorb water is reduced.

It is worth mentioning that desiccant wheel channels cross-sectional can be designed with different shapes. Depending on the governing equations for desiccant wheel simulation, it can be seen that channel perimeter, surface area and hydraulic diameter play important roles on the performance of desiccant wheel. To investigate desiccant channel cross-sectional shapes, it is assumed that perimeters of channels are constant. This assumption means that the mass of desiccant in the channel walls are constant. The value of hydraulic diameter is different and depends on the channel cross-sectional area. The effect of hydraulic diameter on the latent and sensible effectiveness of wheels is illustrated in Figures 10 and 11. Depending on the velocity, there is an optimum hydraulic diameter from which maximum value of latent effectiveness can be obtained. Also sensible effectiveness is reduced by increasing hydraulic diameter.

8. CONCLUSION

A mathematical model based on the transient coupling of heat and mass transfer for desiccant wheel is presented. The governing equations are numerically solved to estimate its performance in different geometrical conditions. The numerical results fall well within the range of experimental measurements. Effect of length, ratio of dehumidification to regeneration and channels hydraulic diameter on the performance of

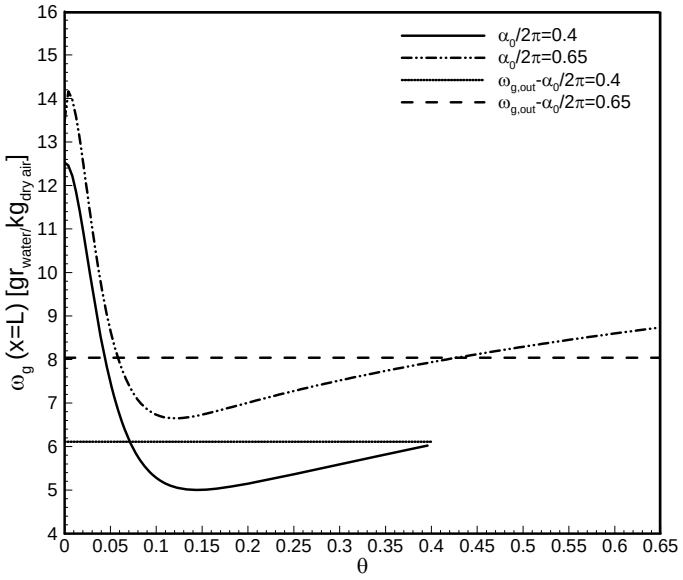

Figure 9. Output air humidity ratio during dehumidification.

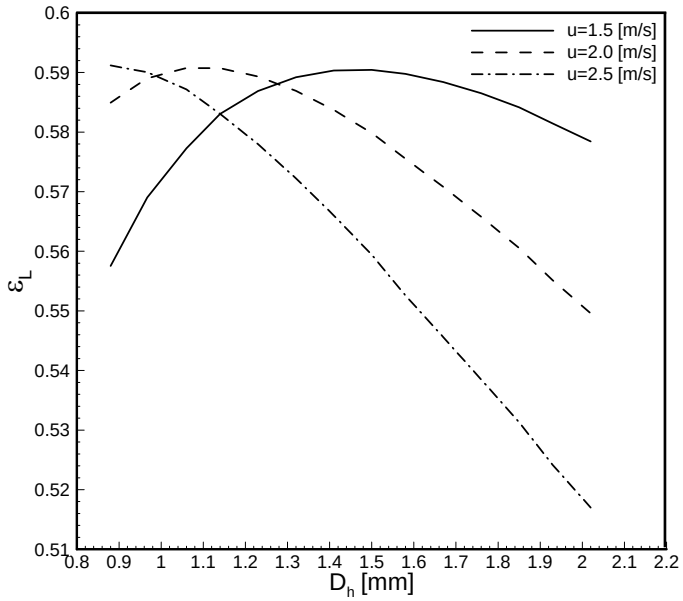

Figure 10. Latent effectiveness under various hydraulic diameter of desiccant wheel.

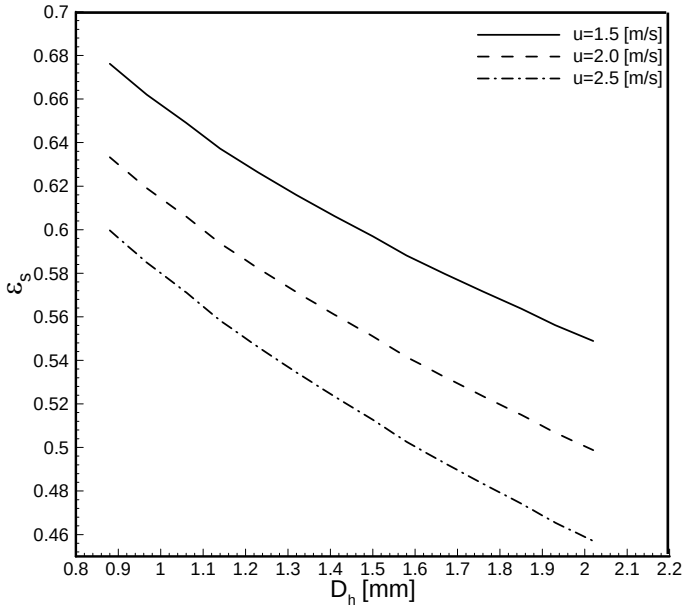

Figure 11. Sensible effectiveness under various hydraulic diameter of desiccant wheel.

desiccant wheel are investigated. There is an optimum value for the ratio of dehumidification to regeneration area which depends on rotational speed. As an example for N = 0.6 rpm the optimum value of α_0 is equal to 0.87 π (see Figure 7). This value is decreased by reducing rotational speed. Also the optimum value of hydraulic diameter depends on air velocity. For u = 1.5 m/s, the optimum hydraulic diameter is equal to 1.5 mm.

9. NOMENCLATURE

A_{duct}	Cross-sectional area of desiccant wheel element (m²)
C	Constant in sorption curve
C_p	Specific heat (kJ $kg^{-1}K^{-1}$)
D_h	Hydrodynamic diameter of a duct (m)
D_s	Surface diffusivity (m^2 s^{-1})
f	Fraction of desiccant in the wheel material
h	Convective heat transfer coefficient (W m^{-2} K^{-1})
h_m	Convective mass transfer coefficient (kg m^2 s^{-1})
k	Thermal conductivity (W m^{-1} K^{-1})
L	Length of duct (m)
Le	Lewis number
$\dot{m}$	Mass flow rate of air stream (kg s^{-1})
N	Rotational speed (rpm)
P	Pressure (Pa)
P_{duct}	Duct perimeter (m)
Q_{sor}	Adsorption heat (kJ kg^{-1})
R	Wheel radius (m)
T	Temperature (˚C)
u	Velocity of air stream (m s^{-1})
W	Water uptake in desiccant (kg water/kg dry desiccant)

Greek Letters

α	Angle (rad)
α_0	Dehumidification angle (rad)
τ	Tortuosity factor
θ	Dimensionless angle (rad/2π)
ε_l	Dehumidification effectiveness
ε_s	Sensible effectiveness
ε_t	Total porosity
ϕ	Relative humidity
δ	Half thickness of duct (m)
ω	Humidity ratio (kg moisture/kg dry air)
ρ	Density (kg m^{-3})

Subscript

α	Dry air
ci	Cool Inlet (process) air stream
d	Desiccant
DA	Dry Air
DD	Dry Desiccant
eff	Effective
eq	Equilibrium content
g	Gas
hi	Hot Inlet (regeneration) air stream
max	Maximum value
min	Minimum value
out	Outlet
p	Process
v	Vapor
w	water

10. REFERENCES

1. ASHRAE 1997, "ASHRAE Handbook-Fundamental", American Society of Heating, Refrigeration and Air-Conditioning Engineers INC, Atlanta, GA, U.S.A., Chapter 22, (2001).
2. Pasdar Shahri, H., Heidarinejad, G. and Delfani, S., "Thermodynamic Simulation of Desiccant Cooling Cycles Performance", ***15th Annual (International) Conference on Mechanical Engineering***, (In Persian), Amirkabir University of Technology, Tehran, Iran, (May 15-17, 2007).
3. Pesaran, A. and Mills, A. F., "Moisture Transport in Silica Gel Packed Bed I. Theoretical Study", ***Int. J. Heat Mass Transfer***, Vol. 30, (1987), 1037-1049.
4. Pesaran, A. and Mills, A. F., "Moisture Transport in Silica Gel Packed Bed II. Experimental Study", ***Int. J. Heat Mass Transfer***, Vol. 30, (1987), 1051-1060.
5. Van Den Bulck, E., Mitchell, J. W. and Klein, S. A., "Design Theory for Rotary Heat and Mass Exchangers, II. Effectiveness-Number-of-Transfer-units Method for Rotary Heat and Mass Exchangers", ***Int. J. Heat Mass Transfer***, Vol. 28, (1985), 1587-1595.
6. Zheng, W. and Worek, W. M., "Numerical Simulation of Combined Heat and Mass Transfer Process in a Rotary Dehumidifier", ***Numerical. Heat Transfer Part A***, Vol. 23, (1993), 211-232.
7. Majumdar, P., "Heat and Mass Transfer in Composite Desiccant Pore Structures for Dehumidification", ***Solar Energy***, Vol. 62, (1998), 1-10.
8. Simonson, C. J. and Besant, R. W., "Energy Wheel Effectiveness. Part I: Development of Dimensionless Groups", ***Int. J. Heat Mass Transfer***, Vol. 42, (1999) 2161-2170.
9. Simonson, C. J. and Besant, R. W., "Energy Wheel Effectiveness. Part II: Correlations", ***Int. J. Heat Mass Transfer***, Vol. 42, (1999), 2171-2185
10. Kodama, A., Hirayama, T., Goto, M., Hirose, T. and Critoph, R. E., "The Use of Psychometric Charts for the Optimization of a Thermal Swing Desiccant Wheel", ***Applied Thermal. Engineering***, Vol. 21, (2001), 1657-1674.
11. Niu, J. L. and Zhang, L. Z., "Effects of Wall Thickness on the Heat and Moisture Transfers in Desiccant Wheels for Air Dehumidification and Enthalpy Recovery", ***Int. Communication Heat Mass Transfer***, Vol. 29, (2002),

255-268.
12. Niu, J. L. and Zhang, L. Z., "Performance Comparisons of Desiccant of Desiccant Wheels for Air Dehumidification and Enthalpy Recovery", ***Applied Thermal. Engineering***, Vol. 22, (2002), 1347-1367.
13. Sphaier, L. A. and Worek, W. M., "Analysis of Heat and Mass Transfer in Porous Sorbents used in Rotary Regenerators", ***Int. J. Heat and Mass Transfer***, Vol. 47, (2004), 3415-3430.
14. Sphaier, L. A. and Worek, W. M., "The Effect of Axial Diffusion in Desiccant and Enthalpy Wheel", ***Int. J. Heat and Mass Transfer***, Vol. 49, (2006), 1412-1419.
15. Camargo, J. R., Godoy, E. and Ebinuma, C. D., "An Evaporative and Desiccant Cooling System for Air Conditioning in Humid Climates", ***Journal of Brazilian Society of Mechanical Engineering***, Vol. 27, (2005), 243-247.
16. Pahlavanzadeh, H. and Zamzamian, A., "A Mathematical Model for a Fixed Desiccant Bed Dehumidifier Concerning Ackermann Correction Factor", ***Iranian Journal of Science and Technology***, Transaction B, Engineering, Vol. 30, (2006), 353-362.
17. Bejan, A. "Convection Heat Transfer", John Wiley and Sons, Vol. 3rd ed., INC, New York, U.S.A., (2004).